J Biomol NMR (2008) 41:121–125
DOI 10.1007/s10858-008-9247-1

COMMUNICATION

MAS solid state NMR of RNAs with multiple receivers

Christian Herbst · Kerstin Riedel · Yvonne Ihle · Jörg Leppert · Oliver Ohlenschläger · Matthias Görlach · Ramadurai Ramachandran

Received: 3 March 2008 / Accepted: 1 May 2008 / Published online: 31 May 2008
© Springer Science+Business Media B.V. 2008

In the study of biomolecular systems, magic angle spinning (MAS) solid state NMR is emerging as a powerful complementary tool to X-ray crystallography and solution state NMR. Making use of the distance and torsion angle constraints extracted in the solid state the structural characteristics of many biologically interesting systems have been elucidated via MAS solid state NMR recently (Castellani et al. 2002; Jaroniec et al. 2002; Rienstra et al. 2002; Luca et al. 2003; Tycko 2003; Krabben et al. 2004; Zech et al. 2005; Iwata et al. 2006; Egawa et al. 2007; Goldbourt et al. 2007). Homo- and heteronuclear distances involving ^{13}C and ^{15}N nuclei with well resolved isotropic chemical shifts are commonly used in MAS solid state NMR based structural studies. Although ^{1}H resonances are generally broad due to strong homonuclear dipolar couplings, the possibilities for extracting short range ^{1}H–^{1}H distance estimates from fully protonated (^{13}C, ^{15}N) labelled peptide/protein samples have been demonstrated recently (de Boer et al. 2002; Lange et al. 2002, 2003, 2005; Tycko and Ishii 2003; Reif et al. 2003). This approach exploits the improved spectral resolution seen in ^{15}N and ^{13}C spectra and involves ^{1}H–^{1}H dipolar coupling mediated chemical shift correlation of the low γ nuclei. Cross-peak intensities seen in such data, commonly referred to as CHHC, CHHN, NHHN and NHHC spectra, are related to the spatial proximity of the protons that are directly attached to the corresponding nuclei observed in the two dimensions. Our recent studies (Riedel et al. 2005a, 2006) indicate that NHHN, CHHC and NHHC type experiments also hold considerable potential in the structural studies of RNAs that play a critical role in many biological processes and exhibit a variety of secondary and tertiary structural features. Duplex regions arising from consecutive formation of hydrogen bonded base pairs are commonly found in RNA. Hence, the identification of the hydrogen bonded base-pairs and the characterisation of the underlying hydrogen bonding patterns is of critical importance in the study of RNA. As different canonical and non-canonical base-pairing schemes encountered in nucleic acids are characterised by topologically different networks of strong proton–proton dipolar couplings, it has been demonstrated that the characterisation of the hydrogen bonding networks in RNAs can be effectively carried out via NHHN and NHHC type of experiments (Riedel et al. 2005a). In addition, it has also been shown that ^{1}H–^{1}H dipolar coupling mediated ^{13}C–^{13}C chemical shift correlation experiments can facilitate the characterisation of the glycosidic torsion angle χ, the sugar pucker and the helical regions of RNAs (Riedel et al. 2006). Hence, data from NHHN, CHHC and NHHC type experiments are critically important in RNA structural studies. Currently, the different proton–proton dipolar coupling mediated $^{15}N/^{13}C$ chemical shift correlation experiments are carried out individually and, hence, considerable amount of spectrometer time is required to generate data with good signal-to-noise ratio. In this communication an efficient approach for the simultaneous collection of these different MAS solid state NMR data sets is presented. The efficacy of the approach is demonstrated using an RNA composed of 97 CUG repeats, $(CUG)_{97}$, a system that is under investigation

Electronic supplementary material The online version of this article (doi:10.1007/s10858-008-9247-1) contains supplementary material, which is available to authorized users.

C. Herbst · K. Riedel · Y. Ihle · J. Leppert · O. Ohlenschläger · M. Görlach · R. Ramachandran (✉)
Research group Biomolecular NMR spectroscopy, Leibniz Institute for Age Research, Fritz Lipmann Institute, Beutenbergstr. 11, 07745 Jena, Germany
e-mail: raman@fli-leibniz.de

in our laboratory (Riedel et al. 2004, 2005a, 2005b, 2006; Riedel 2007, Leppert et al. 2004).

The RF pulse sequence employed for generating ^{1}H–^{1}H dipolar coupling mediated chemical shift correlation of ^{13}C/^{15}N nuclei is shown in Fig. 1. The initial transverse ^{13}C/^{15}N magnetisation prepared by the first cross-polarisation (CP) step is allowed to evolve under ^{1}H decoupling during the t_1 period. The second CP step transfers the t_1 modulated ^{13}C/^{15}N magnetisation back to the protons. The proton magnetisation is then flipped to the z axis and longitudinal ^{1}H magnetisation exchange mediated by proton–proton dipolar couplings is allowed to take place during the proton spin diffusion (Lange et al. 2003; Riedel et al. 2005a, 2006) period τ_{mix}. The proton magnetisation at the end of τ_{mix} is rotated back to the transverse plane. The final CP transfers the polarisation from the protons to the ^{13}C/^{15}N nuclei for simultaneous detection in t_2 using the multiple receiver capabilities in the current generation of spectrometers. The experiment is typically carried out with a very short CP contact time and proton spin diffusion mixing time τ_{mix} to minimise relayed magnetisation transfers during CP and τ_{mix}. Cross-peaks with appreciable intensities are expected only between proton-attached ^{13}C/^{15}N sites that are connected by ^{1}H–^{1}H distances of less than $\sim$3 Å. It is worth mentioning that when the different experiments are carried out individually the HC and HN transfer times can be optimised independently at any given spinning speed. Typically, the HC transfer requires a shorter CP contact time compared to the HN transfer. At the spinning speed of 25,000 Hz employed in this study, a CP contact time of 200 μs was found experimentally to be optimal to achieve satisfactory transfer to both the ^{15}N and ^{13}C nuclei. With such short CP contact times employed in this work, we do not observe any major signal losses during simultaneous H -> N, C cross-polarisations. The $\{(90)_x - (k-1)t_1 - (90)\phi_4\}$ sandwich of pulses and delay applied in the ^{13}C channel is eliminated when the required ^{15}N and ^{13}C ω_1 spectral widths are identical. When the ^{15}N and ^{13}C ω_1 spectral width requirements are different, the chemical shift evolution of ^{15}N is started first, as the ^{15}N spectral width is typically smaller, and during the time interval $(k-1)t_1$, when the ^{15}N magnetisation is evolving, the ^{13}C magnetisation is kept in the z state. The ratio of the ^{15}N and ^{13}C ω_1 spectral widths is controlled by the parameter k. Standard phase cycling procedures were employed to select the desired coherence transfer pathway and quadrature detection in the t_1 dimension is achieved via the States procedure (States et al. 1982). For each increment in t_1, four sets of data were acquired and processed, as described in Table 1, to separate the signals arising from ^{15}N and ^{13}C chemical shift evolutions in t_1 (Sorenson 1990; Farmer II 1991; Ramachandran et al. 1996). The RNA sample was prepared using appropriately labelled ribonucleoside triphosphates as described earlier (Leppert et al. 2004). A hydrated, undiluted $\{^{15}$N, ^{13}C$\}$ labelled RNA sample of $(CUG)_{97}$ ($\sim$7 mg) was used in the experiments carried out at a spinning speed of 25,000 Hz and with cooling air kept at a temperature of ~ -50°C on a 500 MHz wide-bore Bruker Avance III solid state NMR spectrometer equipped with a 2.5 mm triple resonance probe. The processing of the NMR data was carried out with the NMRpipe software (Delaglio et al. 1995).

^{1}H–^{1}H dipolar coupling mediated isotropic ^{15}N/^{13}C chemical shift correlation spectra of the uniformly $\{^{15}$N, ^{13}C$\}$ labelled sample of $(CUG)_{97}$ obtained at a spinning speed of 25,000 Hz using a short proton spin diffusion

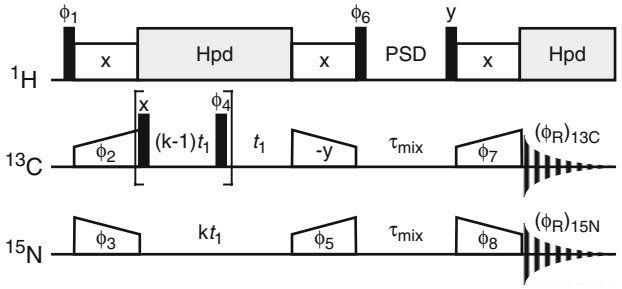

Fig. 1 RF pulse sequence employed in this work. For the case where the ^{15}N and ^{13}C ω_1 spectral width requirements are different, the RF pulse and the receiver phases were cycled as: ϕ_1 = (y, −y); ϕ_2 = (y, y, −y, −y); ϕ_3 = (y, y, −y, −y); ϕ_4 = (16* x, 16* −x); ϕ_5 = (16* −y, 16* y); ϕ_6 = (4* −y, 4* y); $\phi_7 = \phi_8$ = (8* −y, 8* y); $(\phi_R)_N = (\phi_R)_C$ = (x, −x, −x, x, −x, x, x, −x, −x, x, x, −x, x, −x, −x, x, −x, x, x, −x, x, −x, −x, x, −x, x, x, −x, -x, x, −x, x, x, −x). For the case where the ^{15}N and ^{13}C ω_1 spectral widths are identical, the $\{(90)_x - (k-1)t_1 - (90)\phi_4\}$ sandwich in the ^{13}C channel is not applied and the RF pulse and the receiver phases were cycled as: ϕ_5 = −y; $(\phi_R)_N = (\phi_R)_C$ = (x, −x, −x, x, −x, x, x, −x, −x, x, x, −x, x, −x, −x, x) with the other RF pulse phases defined as before. High power ^{1}H decoupling via the SPINAL 64 (Fung et al. 2000; De Paepe et al. 2003) scheme was employed in t_1 and t_2 time periods and phase sensitive 2D spectra were generated as described in the literature (States et al. 1982). The ^{13}C and ^{15}N signals were acquired in t_2 using the corresponding receivers in the two channels

Table 1 Phase cycling used for quadrature detection in t_1 and for seperating signals arising from ^{13}C and ^{15}N chemical shift evolutions in t_1

Data set	ϕ_2 (ϕ_4)	ϕ_3	^{13}C signal	^{15}N signal
1	ϕ_2 (ϕ_4)	ϕ_3	$(N+P)_{t_1}$	$(N+P)_{t_1}$
2	ϕ_2 (ϕ_4) + 90°	ϕ_3 + 90°	$(N-P)_{t_1}$	$(N-P)_{t_1}$
3	ϕ_2 (ϕ_4) + 180°	ϕ_3	$-(N+P)_{t_1}$	$(N+P)_{t_1}$
4	ϕ_2 (ϕ_4) + 270°	ϕ_3 + 90°	$-(N-P)_{t_1}$	$(N-P)_{t_1}$

For obtaining CHHC and CHHN spectral data involving ^{13}C isotropic chemical shift evolution in t_1, the data set (1–3) gives the real part (N + P) and the data set (2–4) yields the imaginary part (N − P) of the signal in t_1. For obtaining NHHC and NHHN spectra, involving ^{15}N isotropic chemical shift evolution in t_1, (1 + 3) and (2 + 4) yield the real and imaginary parts in t_1

mixing time of 160 μs and a 2.5 mm MAS rotor are shown in Fig. 2a–d. The resonance assignments indicated are based on our recent studies (Riedel et al. 2005b). The spectral characteristics observed are as expected for a helical RNA with GC base-pairs and glycosidic torsion angle χ in *anti* and are consistent with the data presented earlier (Riedel et al. 2005a, 2006). Due to the high spinning speed employed, the structurally important C8/C6 (aromatic) $\leftrightarrow$ C2′/C3′ (ribose) cross-peaks are seen with good signal-to-noise ratio in the CHHC spectrum (Fig. 2a). It is worth mentioning that it is possible to extract structurally meaningful conclusions, from data such as the CHHC spectrum, not only by the presence but also from the absence of certain cross-peaks. For example, the absence of cross-peaks between the aromatic and sugar C1′ carbons directly indicates a χ angle, describing the relative orientation of the base and the sugar moiety across the glycosidic bond, in the *anti* range (Riedel et al. 2006). The cross-peak between the guanine imino and cytosine amino nitrogens arising from the spatial proximity of the corresponding protons in a GC base-pair is seen in the NHHN spectrum (Fig. 2d). The spectral characteristics of CHHN (Fig. 2b) and NHHC (Fig. 2c) data are also as expected. With the χ angle in the *anti* range, the intra-nucleotide distance between the guanine H1′ and the non-hydrogen bonded guanine amino proton is larger than 4 Å, hence, an intra-nucleotide cross-peak between the guanine amino nitrogen and the ribose C1′ carbon is not expected in the NHHC/CHHN spectra. However, it is well known from solution state NMR studies that an A-form helix leads to the spatial proximity of the non-hydrogen-bonded G amino proton with the ribose H1′ proton of the $n + 1$ neighbouring nucleotide in the same strand (Heus and Pardi 1991). Hence, the presence of a cross-peak between the guanine amino nitrogen and the ribose C1′ carbon in the NHHC and CHHN spectra of $(CUG)_{97}$ is consistent with

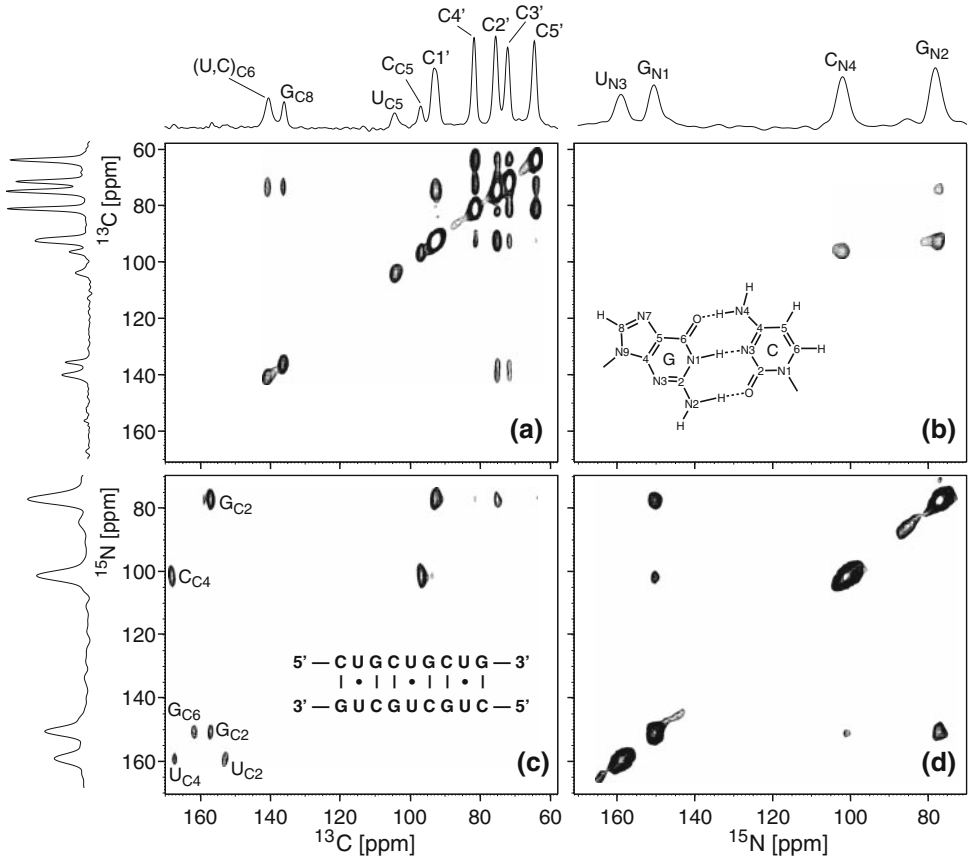

Fig. 2 Experimental CHHC (**a**), CHHN (**b**), NHHC (**c**) and NHHN (**d**) MAS solid state NMR spectra of $(CUG)_{97}$ RNA generated via the pulse sequence given in Fig. 1 employing ^{15}N and ^{13}C ω_1 spectral widths of 8,333.3 Hz and 25,000 Hz, respectively, a spinning speed of 25,000 Hz, data acquisition in the direct dimension of 10 ms for ^{13}C and 12 ms for ^{15}N, ramp CP contact times of 200 μs, a recycle time of 2 s, 40 t_1 increments (corresponding to t_1 acquisition times of 1.6 ms and 4.8 ms, respectively, in the ^{13}C and ^{15}N dimensions) with 256 transients per t_1 increment and a τ_{mix} of 160 μs. The assignments of the different resonances are also indicated in the 1D spectra collected with short CP contact times. A schematic representation of the double stranded $(CUG)_{97}$ employed in this study and the GC Watson–Crick base-pairing scheme are also shown. Additional details of spectral processing and representative 1D slices taken from the 2D spectra are given in the Supplementary material

the A-form helical conformation of this RNA (Riedel et al. 2006). The spatial proximity between the non-hydrogen bonded amino proton of the cytosine and the cytosine aromatic H5 proton results in the appearance of the strong cross-peak observed between the corresponding amino nitrogen and the C5 carbon in the NHHC/CHHN spectra, permitting the assignment of these resonances. The signal intensities seen in the CHHN spectrum, with ^{15}N detection in the t_2 dimension, are typically weaker than that observed in the NHHC spectrum. Although cross-peaks in the CHHC, CHHN, NHHN and NHHC spectra should arise in principle between heteronuclei attached to spatially proximal protons, the NHHC spectrum shows a number of cross-peaks involving the imino and amino nitrogens and carbons with no attached protons. Such correlations arise due to the fact that during the final CP step the cross-polarisation to the quaternary carbons predominantly arises from protons that are not strongly coupled to a ^{13}C spin, such as the imino and amino protons (van Rossum et al. 2000). With short CP contact time typically employed in these studies, such cross-peaks originate mainly from short range 2-bond intra-nucleotide heteronuclear dipolar interactions (Fig. 2c) and, hence, provide a convenient alternative approach for the assignment of many of the important quaternary carbon resonances in RNAs. A short HC transfer time after proton mixing can lead to a reduction in the transfer of proton polarisation to non-protonated ^{13}C nuclei. However, at the spinning speed of 25,000 Hz it is seen that using a very short HC transfer time leads to a reduction in the intensities of other signals of interest. An optimised value of 200 μs was employed for the CP contact times. Cross-peaks arising from inter-strand heteronuclear dipolar interactions and reflecting the presence of hydrogen-bonded base-pairs can be clearly seen in experiments carried out with longer contact time for the third CP step (data not shown).

Simultaneous collection of different ^{1}H–^{1}H dipolar coupling mediated chemical shift correlation data sets of (^{13}C, ^{15}N) labelled RNAs provides in a single experiment a variety of structural information and resonance assignments. The availability of such complementary data sets may also be required for undertaking a detailed quantitative analysis of the observed cross-peak intensities as a function of the mixing time. For example, an analysis of the observed cross-peak intensities in the NHHN spectrum (Fig. 2d) considering a dipolar network involving only protons connected to ^{15}N nuclei can lead to erroneous results as the NHHC spectrum (Fig. 2c) clearly reveals the presence of a much larger homo- and heteronuclear dipolar spin network involving protons connected to both ^{15}N and ^{13}C nuclei. Hence, the simultaneous evaluation of all the relevant cross-peak intensities in the different data sets may be necessary for extracting ^{1}H–^{1}H distances quantitatively.

The possibilities for reducing data acquisition times by the simultaneous collection of the signals arising from different nuclei in the direct dimension t_2 was demonstrated recently in the context of solution state NMR studies (Kupce et al. 2006). The present work, dealing with MAS solid state NMR studies, extends this approach further and illustrates how several multidimensional correlation spectra can be much more efficiently collected. It makes use of the capabilities in the current generation of NMR spectrometers for simultaneously collecting the signals from different nuclear species in the acquisition dimension. Additionally, suitable RF pulse phase cycling procedures are employed for generating the phase- sensitive data sets such that the signals arising from ^{15}N and ^{13}C evolutions in t_1 are also simultaneously obtained. It is worth mentioning that it is often necessary to work with small quantities of fully labelled materials as experiments carried out at high MAS frequencies to minimise the deleterious effects of CSAs, e.g. on the aromatic carbons of the nucleotide bases, would necessarily require the use of small volume rotors. Considering the fact that the sample has to be also fully hydrated to get the proper RNA fold (Leppert et al. 2004), the amount of labelled sample that can be used in these experiments will be very limited. Under these circumstances, the approach presented leads to considerable savings in time in collecting different proton–proton dipolar coupling mediated ^{15}N/^{13}C chemical shift correlation data with good signal-to-noise ratio. Although demonstrated in the context of RNA, the MAS solid state NMR method outlined here can be equally employed to reduce spectral data acquisition times in the study of peptides/proteins.

Acknowledgements This study has been funded in part by a grant from the Deutsche Forschungsgemeinschaft (grant no.: GO474/6-1). The referees are also thanked for their useful comments on the original manuscript.

References

Castellani F, van Rossum B, Diehl A, Schubert M, Rehbein K, Oschkinat H (2002) Structure of a protein determined by solid-state magic-angle-spinning NMR spectroscopy. Nature 420: 98–102

de Boer I, Bosman L, Raap J, Oschkinat H, de Groot HJ (2002) 2D 13C–13C MAS NMR correlation spectroscopy with mixing by true 1H spin diffusion reveals long-range intermolecular distance restraints in ultra high magnetic field. J Magn Reson 157: 286–291

De Paepe G, Lesage A, Emsley L (2003) The performance of phase modulated heteronuclear dipolar decoupling schemes in fast magic-angle-spinning nuclear magnetic resonance experiments. J Chem Phys 119:4833–4841

Delaglio F, Grzesiek S, Vuister GW, Zhu G, Pfeifer J, Bax A (1995) NMRPipe: a multidimensional spectral processing system based on UNIX pipes. J Biomol NMR 6:277–293

Egawa A, Fujiwara T, Mizoguchi T, Kakitani Y, Koyama Y, Akutsu H (2007) Structure of the light-harvesting bacteriochlorophyll c assembly in chlorosomes from Chlorobium limicola determined by solid-state NMR. Proc Natl Acad Sci USA 104:790–795

Farmer BT II (1991) Simultaneous [^{13}C, ^{15}N]-HMQC, a pseudo-triple-resonance experiment. J Magn Reson 93:635–641

Fung BM, Khitrin AK, Ermolaev K (2000) An improved broadband decoupling sequence for liquid crystals and solids. J Magn Reson 142:97–101

Goldbourt A, Gross BJ, Day LA, McDermott AE (2007) Filamentous phage studied by magic-angle spinning NMR: Resonance assignment and secondary structure of the coat protein in Pf1. J Am Chem Soc 129:2338–2344

Heus HA, Pardi A (1991) Novel 1H nuclear-magnetic-resonance assignment procedure for RNA duplexes. J Am Chem Soc 113:4360–4361

Iwata K, Fujiwara T, Matsuki Y, Akutsu H, Takahashi S, Naiki H, Goto Y (2006) 3D structure of amyloid protofilaments of beta(2)-microglobulin fragment probed by solid-state NMR. Proc Natl Acad Sci USA 103:18119–18124

Jaroniec CP, MacPhee CE, Astrof NS, Dobson CM, Griffin RG (2002) Molecular conformation of a peptide fragment of transthyretin in an amyloid fibril. Proc Natl Acad Sci USA 99:16748–16753

Krabben L, van Rossum BJ, Castellani F, Bocharov E, Schulga AA, Arseniev AS, Weise C, Hucho F, Oschkinat H (2004) Towards structure determination of neurotoxin II bound to nicotinic acetylcholine receptor: a solid-state NMR approach. Febs Lett 564:319–324

Kupce E, Freeman R, John BK (2006) Parallel acquisition of two-dimensional NMR spectra of several nuclear species. J Am Chem Soc 128:9606–9607

Lange A, Luca S, Baldus M (2002) Structural constraints from proton-mediated rare-spin correlation spectroscopy in rotating solids. J Am Chem Soc 124:9704–9705

Lange A, Seidel K, Verdier L, Luca S, Baldus M (2003) Analysis of proton–proton transfer dynamics in rotating solids and their use for 3D structure determination. J Am Chem Soc 125: 12640–12648

Lange A, Becker S, Seidel K, Giller K, Pongs O, Baldus M (2005) A concept for rapid protein-structure determination by solid-state NMR spectroscopy. Angew Chem Int Ed 44:2089–2092

Leppert J, Urbinati CR, Hafner S, Ohlenschlager O, Swanson MS, Gorlach M, Ramachandran R (2004) Identification of NH…N hydrogen bonds by magic angle spinning solid state NMR in a double-stranded RNA associated with myotonic dystrophy. Nucleic Acids Res 32:1177–1183

Luca S, White JF, Sohal AK, Filippov DV, van Boom JH, Grisshammer R, Baldus M (2003) The conformation of neurotensin bound to its G protein-coupled receptor. Proc Natl Acad Sci USA 100:10706–10711

Ramachandran R, Sich C, Grüne M, Soskic V, Brown LR (1996) Sequential assignments in uniformly ^{13}C- and ^{15}N-labelled RNAs: the HC(N, P) and HC(N, P)-CCH-TOCSY experiments. J Biomol NMR 7:251–255

Reif B, Van Rossum BJ, Castellani F, Rehbein K, Diehl A, Oschkinat H (2003) Characterization of ^{1}H–^{1}H distances in a uniformly ^{2}H, ^{15}N-labeled SH3 domain by MAS solid-state NMR spectroscopy. J Am Chem Soc 125:1488–1489

Riedel K, Leppert J, Häfner S, Ohlenschläger O, Görlach M, Ramachandran R (2004) Homonuclear chemical shift correlation in rotating solids via RN_n^ν symmetry-based adiabatic RF pulse schemes. J Biomol NMR 30:389–395

Riedel K, Leppert J, Ohlenschläger O, Görlach M, Ramachandran R (2005a) Characterisation of hydrogen bonding networks in RNAs via magic angle spinning solid state NMR spectroscopy. J Biomol NMR 31:331–336

Riedel K, Leppert J, Ohlenschläger O, Görlach M, Ramachandran R (2005b) TEDOR with adiabatic inversion pulses: Resonance assignments of ^{13}C/^{15}N labelled RNAs. J Biomol NMR 31: 49–57

Riedel K, Herbst C, Häfner S, Leppert J, Ohlenschläger O, Swanson MS, Görlach M, Ramachandran R (2006) Constraints on the structure of (CUG) 97 RNA from magic-angle-spinning solid-state NMR spectroscopy. Angew Chem Int Ed 45:5620–5623

Riedel K (2007) Methoden zur Untersuchung biologischer Moleküle mittels Festkörper-Kernresonanzspektroskopie. Phd Thesis, Friedrich-Schiller-University, Jena

Rienstra CM, Tucker-Kellogg L, Jaroniec CP, Hohwy M, Reif B, McMahon MT, Tidor B, Lozano-Perez T, Griffin RG (2002) De novo determination of peptide structure with solid-state magic-angle spinning NMR spectroscopy. Proc Natl Acad Sci USA 99:10260–10265

Sorenson OW (1990) Aspects and prospects of multidimensional time-domain spectroscopy. J Magn Reson 89:210–216

States DJ, Haberkorn RA, Ruben DJ (1982) A two-dimensional nuclear overhauser experiment with pure absorption phase in four quadrants. J Magn Reson 48:286–292

Tycko R (2003) Applications of solid state NMR to the structural characterization of amyloid fibrils: methods and results. Progr Nucl Magn Reson Spec 42:53–68

Tycko R, Ishii Y (2003) Constraints on supramolecular structure in amyloid fibrils from two- dimensional solid-state NMR spectroscopy with uniform isotopic labeling. J Am Chem Soc 125:6606–6607

van Rossum BJ, de Groot CP, Ladizhansky V, Vega S, de Groot HJM (2000) A method for measuring heteronuclear ^{1}H–^{13}C distances in high speed MAS NMR. J Am Chem Soc 122:3465–3472

Zech SG, Wand AJ, McDermott AE (2005) Protein structure determination by high-resolution solid-state NMR spectroscopy: application to microcrystalline ubiquitin. J Am Chem Soc 127:8618–8626